Journal of Visualization, Vol. 7, No. 4 (2004) 273-280

Instability of Surfactant Solution Flow in a Taylor Cell

Watanabe, K.[*1], Takayama, T.[*2] and Ogata, S.[*3]

*1 Graduate School of Engineering, Tokyo Metropolitan University, Hachiooji-shi, Tokyo, 192-0397, Japan. E-mail: keizo@ecomp.metro-u.ac.jp
*2 Engineering Research Center, Toshiba Carrier Co. Ltd., Fuji-shi, Shizuoka, 410-0395, Japan.
*3 Graduate School of Engineering, Tokyo Metropolitan University, Hachiooji-shi, Tokyo, 192-0397, Japan.

Received 30 March 2004
Revised 28 May 2004

Abstract : The hydrodynamic instability of surfactant solutions between two coaxial cylinders was investigated by using a laser-induced-fluorescence flow visualization technique to clarify the effect of drag-reducing additives on vortex formation in Taylor-Couette flow. The test fluids were Ethoquad O/12 surfactant solutions, which have a gel-like structure called "shear-induced structure" (SIS). Photographs of the formation of Görtler vortices were taken and compared with these of tap water. In the Taylor number range of $1.2\times10^5 \leq Ta \leq 7.1\times10^5$, tap water and 10 ppm surfactant solution flows consisted of Taylor vortices and much smaller Görtler vortices at the rotating inner wall. However, for 50 and 100 ppm surfactant solutions, Taylor vortices were not apparent and Görtler vortices were collapsed. Measurements of the wavelength of Görtler vortices lead to the conclusion that surfactant solutions have a stabilizing effect on Görtler instabilities. This effect depends on surfactant concentration and becomes considerable with increasing acceleration of the inner cylinder.

Keywords : Visualization, Non-Newtonian Flow, Surfactant solutions, Taylor cell, Görtler vortices.

Nomenclature:

L	cylinder height, L = 240 mm
Ri	inner cylinder radius, Ri = 81 mm
Ro	outer cylinder radius, Ro = 120 mm
T	temperature of test fluid
T_a	Taylor number, $Ta = (Ri\ \omega_i{}^2\ \delta^3) / \nu^2$
T_a *	non-dimensional Taylor number, $T_a{}^* = T_a / T_{a\,cri}$
$T_{a\,crit}$	critical Taylor number, $T_{a\,crit} = 4.6\times10^3$
t	time of inner cylinder rotating
t_s	the time for the flow to become stable, t_s = 10800 s
δ	gap width, $\delta = Ri - Ro$ = 39 mm
Γ	aspect ratio, $\Gamma = L / \delta$
$\dot{\gamma}$	shear rate
η	viscosity of test solution
λ_G	Görtler wavelength
ν	kinematic viscosity of tap water
ω_i	angular velocity

1. Introduction

Because of instability, the flow pattern between two coaxial cylinders changes considerably with speed. It is known that the pattern can change to Taylor-Couette flow from rotational Couette flow (Coles, 1965) with an increase in speed, for a Newtonian fluid between a rotating inner cylinder and a stationary outer cylinder. The flow field is ideal for research into the transition process from laminar to turbulent flow because it is slower than other flow systems and the instabilities are well understood. Thus, much theoretical and experimental research on the transition process using this flow field has been carried out for Newtonian fluids since Taylor's work (1923).

In the field of drag reduction, it has been found that surfactant solutions causes drag reduction (Zakin and Chang, 1974) and do not degrade, even at the high shear rate, and thus the surfactant additives can be applied to district heating or cooling systems to save energy. As a consequence, many experimental studies have been done on the flow characteristics of surfactant solutions in a circular pipe. However, there have been few basic experimental studies on the transition from laminar to turbulent flow, which may be considered closely related to the drag-reducing mechanism. As was mentioned earlier, Taylor-Couette flow is an ideal flow field for research on the transition.

Generally speaking, for drag-reducing polymer and surfactant solutions, viscoelasticity is a known factor. In addition, the behavior of surfactant micelles under shear is complicated and hence many problems remain in the determination of the proper constitutive equations.

In previous studies with polymer solutions, the problem of a purely elastic Taylor-Couette instability has been noted. Larson et al. (1990) showed that, for the Oldroyd-B fluid, there exists an inertia-free mode of instability in Taylor-Couette flow. By a linear stability analysis, they showed that secondary toroidal cells occur when the Deborah number De reaches 20, and the result was in agreement with experiments for a solution of 1000 ppm high-molecular-weight polyisobutylene in a viscous solvent. Sadanandan and Sureshkumar (2002) explored analytically the influence of elasticity on the budgets of the vorticity and the kinetic energy associated with the most dangerous disturbance to the plane Poiseuille flow of a model polymer solution of Oldroyd-B fluid. They showed that a stabilizing effect due to the perturbation shear stress that increases monotonically with increasing the elasticity number and a destabilizing influence due to the perturbation normal stress that increases monotonically. Sureshkumar et al. (1994) calculated the bifurcating families corresponding to each one of the two possible non-axisymmetric patterns emerging at the point of criticality, namely the spirals and ribbons, and determined their stability. They showed that the most unstable oscillatory modes are always non-axisymmetric, and transitions to them are probably discontinuous. Although the extensional nature of the fluid does play an important role, the resulting flow pattern in the case are not shown. Groisman and Steinberg (1996) showed that two novel oscillatory flow patterns are observed in small additions of polymers on the character of instability in Couette-Taylor flow experimentally. One of them is essentially due to the fluid elasticity, and the other results from inertial instability modified by the elasticity.

Lee et al. (1995) carried out a flow visualization study to reveal the effect of dilute polymer solutions on the Görtler instability between two cylinders. They showed experimental results in which the Görtler instability is stabilized by the polymer additive, caused by an increase in the local viscosity. Consequently, previous studies have pointed out that the viscoelasticity in a polymer solution increases the critical Taylor number at which a cellular flow is first observed.

However, the formation of Taylor vortices has not been clarified by flow visualization for drag-reducing surfactant additives. Although it has been speculated that transition with a Newtonian fluid is different from that for a viscoelastic fluid, the vortex formation process has not been sufficiently studied.

The objective of this study is to clarify the formation process of Taylor vortices with regard to the effect of surfactant additives on the instability, by using a flow visualization technique.

2. Experimental Apparatus and Method

Test fluid is tap water, and aqueous solutions of oreyl-bishydroxyethl-methy-ammonium ($C_{18}H_{35}N(C_2H_4OH)_2CH_3Cl$, trade name: Ethoquad O/12) at concentration 10, 50 and 100 ppm in comparing with the results of the flow visualization of tap water were tested. To produce the increase of the local viscosity, the sodium salicylate (NaSal) was added as a counter-ion. The concentration ratio of sodium salicylate to Ethoquad O/12 was set at a molar ratio of 1:1.

Figure 1 shows the relationship between the apparent shear viscosity η and the shear rate $\dot{\gamma}$ of the test fluids as measured by a capillary viscometer. The viscosity depends on the shear rate and the concentration of solution because these solutions have a "shear-induced structure" (Ohlendolf et al., 1997) in the low shear rate range. As the shear rate increases, the micelles in the solutions align along the flow direction so that the viscosity becomes smaller. The temperature of the solution was maintained at $T = 13.0 \pm 0.5$°C throughout the experiments because the solutions' rheology is temperature-dependent.

The experimental apparatus, shown in Fig. 2, is a two-coaxial-cylinder system in which the inner cylinder is rotated at a constant speed by a servomotor, and the outer cylinder and end wall are stationary. The height and the gap between the cylinders are $L = 240$ mm and $\delta = 39$ mm, respectively. The radius of the outer cylinder is $R_0 = 120$ mm, since the aspect ratio $\Gamma = (L / \delta)$, is 6.15, six Taylor vortices should appear in the gap. The angular velocity of the inner cylinder ω_i was measured by means of a digital counter. The inner and outer cylinders are made of aluminum and acrylic resin, respectively. An acrylic resin container, filled with tap water to protect the light reflected from the laser sheet, covers the outer cylinder. Test fluids were supplied from a head tank through a nylon tube to prevent contamination by bubbles.

The formation and evolution of counter-rotating vortices close to the inner cylinder wall were examined by means of a laser-induced-fluorescence (LIF) flow visualization technique. A laser beam was directed radially through the center of the cylinders and spread into a vertical laser sheet by a cylindrical lens, illuminating the flow in the vertical plane. The thickness of the sheet was about 5 mm. Test fluids were marked with a fluorescein dye injected upstream of the laser sheet using a syringe, via a 1 mm tube inserted between the cylinders through a hole in the top of the end plate. The most effective method of marking the flow close to the inner cylinder was to slowly bleed dye directly onto the surface of the inner cylinder, and the near-wall vortices entrained the dyed fluid away from to make the vortices visible. It was confirmed, using a capillary viscometer, that there was no change in the viscosity of

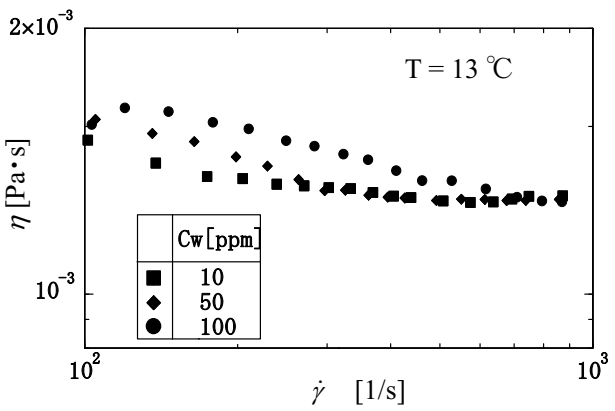

Fig. 1. Shear viscosity for surfactant solution.

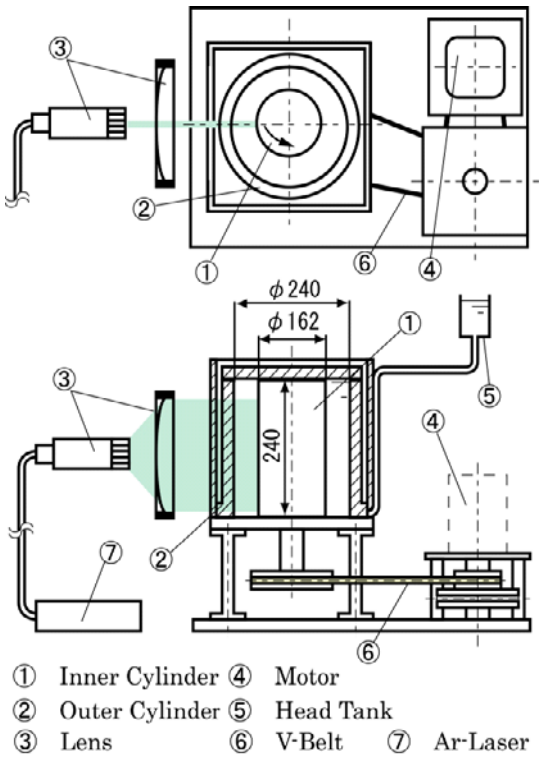

Fig. 2. Experimental apparatus.

the liquid which was mixed with the visualization dye. Visual records of the LIF experiments were made using a video system. The range of non-dimensional Taylor number T_a^*, defined as the ratio of the Taylor number T_a and the critical Taylor number T_{acrit} was $39 \leq T_a^* \leq 236$. Here the Taylor number is defined as $Ta = (Ri\omega_i^2\delta^3) / \nu^2$ where ν is kinematic viscosity. In this paper, we calculated the Taylor number using the viscosity value of tap water. Three acceleration rates were applied to check the effect of acceleration on the formation of Taylor vortices.

3. Experimental Results and Discussions

Figure 3 illustrates the flow conditions of several test fluids in the gap. The time for the flow to become stable was t_s determined using Snyder's equation (Snyder, 1969), as given by

$$t_s \cong 0.15 \frac{L^2}{\nu} \tag{1}$$

where, L and ν are the length of the cylinder and kinematic viscosity, respectively. In this experiment, the time t_s is about 10800 seconds.

As is evident in Fig. 3(a), six Taylor cells appeared in the case of tap water. Observations of the flow confirmed that the boundaries of the Taylor cells did not fluctuate with time and that secondary flow, which had come into contact with both end planes of the inner cylinder, approached the inner wall from the outer one. And the vortex ring was circumferentially uniform. These facts mean that the flow is in a normal mode (Ohlendolf et al., 1997), which is generally the case for the laminar Taylor vortex flow.

Taylor cells also appeared in the case of the 10 ppm surfactant solution, as shown in Fig. 3(b), again exhibiting the normal mode. However, no Taylor cells appeared in the cases of the 50 ppm and 100 ppm solutions shown in Figs. 3(c) and (d), respectively, even after the stabilization time t_s.

How the flow of tap water changes with time is shown in Fig. 4, after rotation of the inner cylinder has started. The manner in which the Görtler vortex is generated, about 40 seconds after rotation starts from the inner wall is confirmed from Fig. 4(a). As the series of photographs show, a

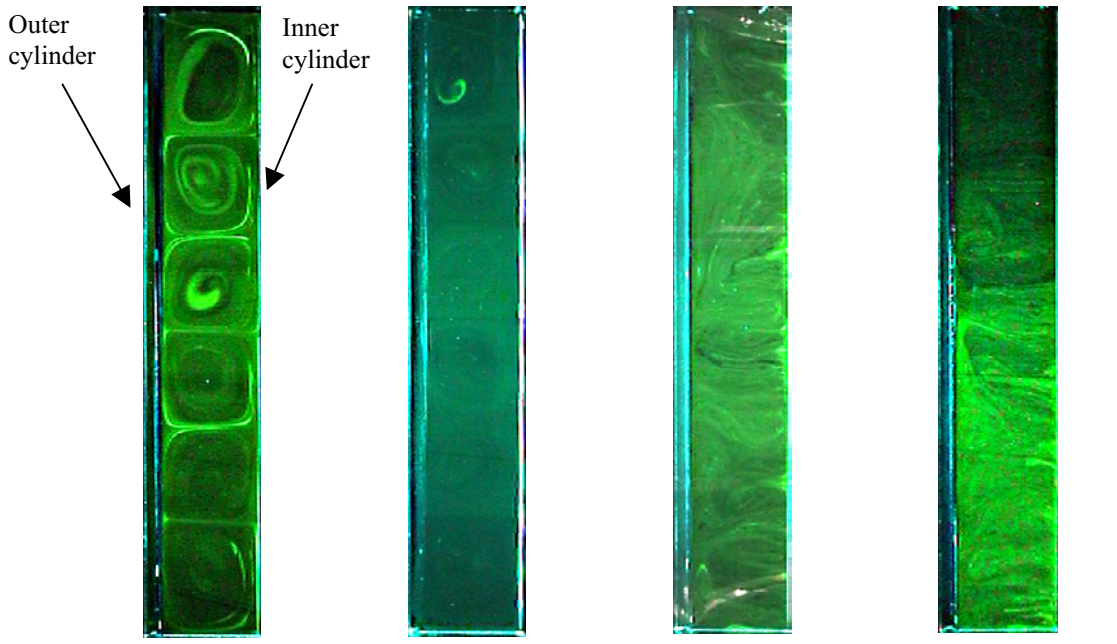

(a) Tap water (b) Cw = 10 ppm (c) Cw= 50 ppm (d) Cw = 100 ppm

Fig. 3. Flow between two coaxial cylinders (Ta^* = 39, dTa^* / dt =232 min^{-1}, T = 13℃).

vortex starts from the inner wall and divides top and bottom after it reaches the outer wall. The Görtler vortex has the shape of a classic mushroom, which consists of a pileus and a stipe. A Taylor cell is soon formed, as seen in Fig. 4(e).

Figure 5(a) shows how a Taylor cell is created for a 100 ppm surfactant solution. The dome (pileus) of the Görtler vortex separates from the main (stipe) part of the vortex in Figs. 5(c) and (d). This separation is related to the fact that the Görtler vortex does not grow and the Taylor cell is not able to form as a result, as illustrated in Fig. 5(e). This separation phenomenon was also observed in 50 ppm surfactant solutions. As stated above, a Görtler vortex does not separate in tap water, as shown in Figs. 4(c) and (d). The range of the maximum shear rate, calculated by applying the mean velocity of Couette flow is $3.6\times10^2 \le \dot{\gamma} \le 8.8\times10^2$. As mentioned with respect to the flow curves in Fig. 1, these results demonstrate that the higher local viscosity prevents development of the vortex in the surfactant solutions.

Figure 6 shows the effect of surfactant concentration on the wavelength of the Görtler vortex. The wavelength was measured by the method of Wei et al.' s (1992), in which the center-to-center distance was measured and two times this value was taken to be the wavelength λ_G. The examples of the definition of λ_G are shown in Figs. 4 and 5, respectively. The experimental values are mean values obtained from 50 to 100 samples, and the error bars in the figure represent 95% confidence levels. The solid line in Fig. 6 is the experimental result for Newtonian fluids obtained by Wei et al., expressed as,

$$\frac{\lambda_G}{R_0} = 31.89\left(\frac{\omega_i{}^2 R_0{}^4}{\nu^2}\right)^{-1/3} \tag{2}$$

(a) 40 s (b) 60 s (c) 70 s (d) 80 s (e) 150 s

Fig. 4. Formation process of Taylor cells for tap water (Ta^* = 39, dTa^*/dt =232 min^{-1}, T = 13℃).

where, R_o, ω_i and ν are the outer cylinder radius, the angular velocity of the inner cylinder and the kinematic viscosity, respectively. Although our experimental data for tap water are above the line, there is a tendency for better agreement at lower Taylor numbers. Wei et al (1992). reported that the wavelength increases with the clearance distance and Eq. (2) applies to small gaps. Because of the wide gap in our experiment, the data for tap water lie above the solid line.

The wavelength of surfactant solutions decreases slowly with T_a^* in comparison to tap water for all these concentrations. This means that the solutions' stabilizing effect on the Görtler instability increases with T_a^* and with surfactant concentration. The effect of inner cylinder acceleration on the wavelength is presented in Fig. 7, which shows only a weak dependence. Counter-ion was added to the surfactant solutions, as described in the previous section, affecting the shear-induced structure of the solutions. Experiments are carried out to visualize the formation process of the Taylor cell of the solution without counter-ion because it is known that a cationic surfactant forms long threadlike micelles in aqueous solution by adding sodium salicylate or cetyltrimethylammonium and counter-ion cause a micelle network to form. The threadlike micelles make concentrated entanglement networks to show pronounced viscoelastic behavior as well as concentrated polymer systems (Imai and Shikata, 2001). However, a responsible mechanism for the longest relaxation mode of the threadlike micellar system is different from that of the polymer system.

Gupta et al. (2002) reported the results of a linear stability analysis of the Taylor Couette of non-Brownian fiber suspensions that irrespective of the closure approximation, used the fiber additives suppress the centrifugal Taylor Couette instability, i.e., the critical Reynolds number increases with fiber volume fraction and aspect ratio. The enhanced stabilizing cab is attributed to the fact that the suspension develops negative first and second normal stresses in the flow system. Moreover, the dynamic interaction between turbulence and the viscoelastic behavior play a significant role in the stability (Arora et al., 2002). Generally speaking, the influence of the

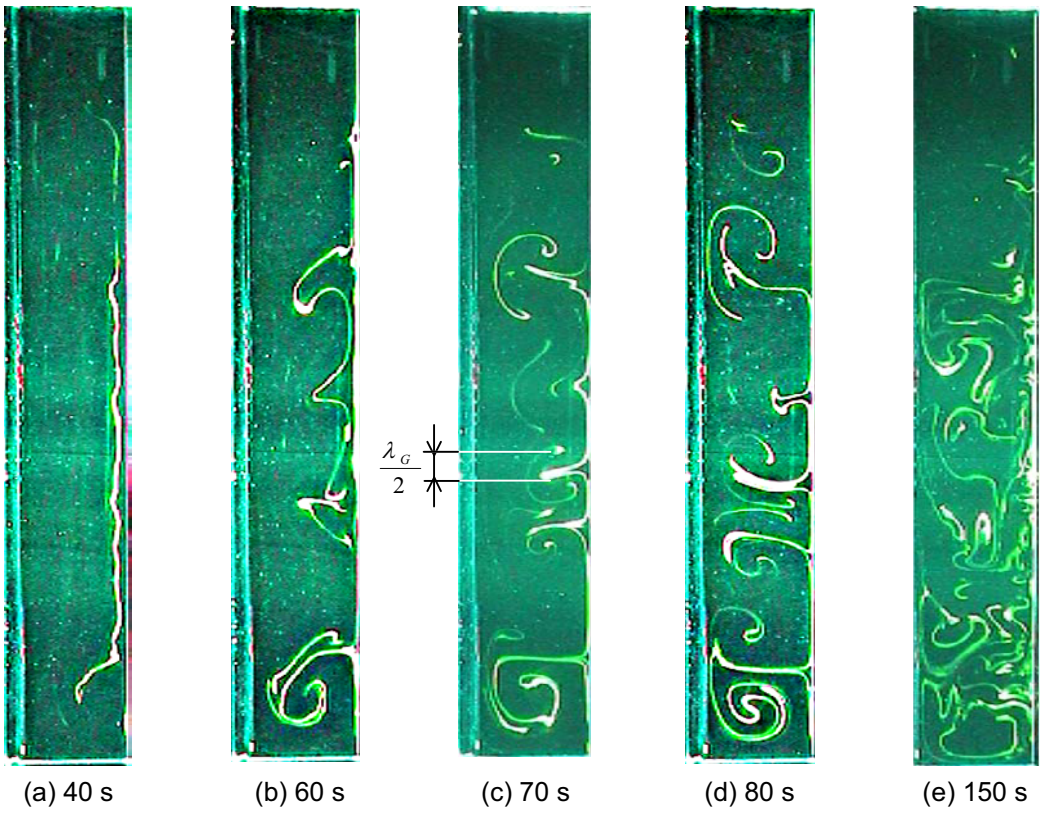

(a) 40 s (b) 60 s (c) 70 s (d) 80 s (e) 150 s

Fig. 5. Formation process of Taylor cells for 100 ppm surfactant solution (Ta^* = 39, dTa^*/dt =232 min^{-1}, T = 13℃).

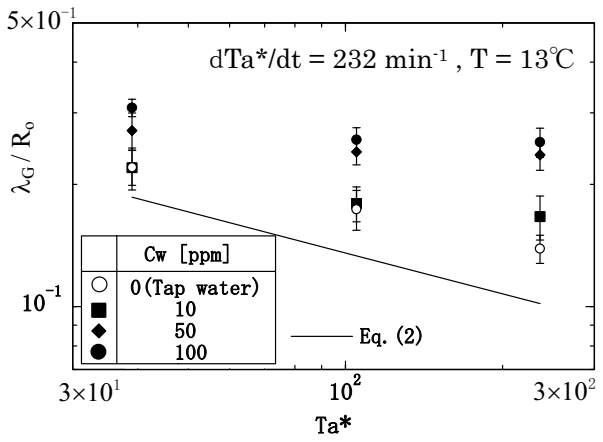

Fig. 6. Görtler wavelength for surfactant solutions.

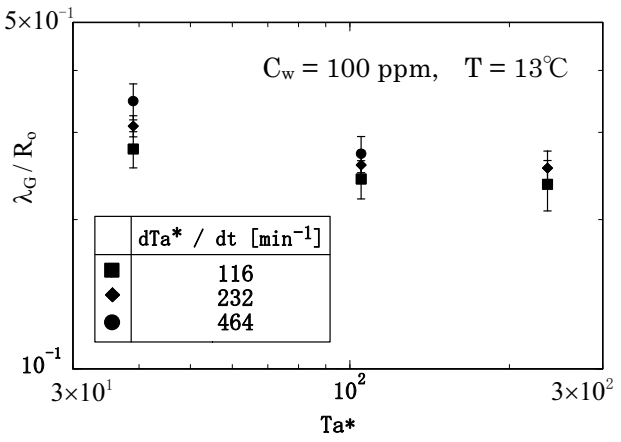

Fig. 7. Effect of acceleration for Görtler wavelength.

viscoelastic behavior in the shear-induced structure on the stability of the forming process of Taylor cells is relatively less understood at present.

Figure 8 shows the flow visualization results. As described earlier in this paper, Taylor cells did not appear for 100 ppm solutions with counter-ion added. However, the Taylor cells clearly form in the absence of counter-ion, as shown in Fig. 8(b). Thus, this result suggests that increasing the local viscosity due to a shear-induced structure causes a stabilizing effect on the Görtler instability. As a result, Taylor cells do not appear in the 50 and 100 ppm surfactant solution.

4. Conclusion

The effect of drag-reducing surfactant additives on the formation of Taylor cells in Taylor-Couette flow was investigated by means of a laser-induced-fluorescence (LIF) flow visualization technique. Visual observations reveal that Taylor cells were not formed in 50 or 100 ppm solution in spite of their forming in tap water and 10 ppm surfactant solutions. Measurements of the wavelength of the Görtler vortices lead to the conclusion that the stabilizing effect on the Görtler instability increases with surfactant concentration. It is thought the stabilizing effect is caused by an increase in local viscosity which is the result of a shear-induced structure at the micelle level, because Taylor cells were formed in 100 ppm solution without counter-ion, although they were not formed in the same solutions with counter-ion.

Acknowledgements

The authors would like to acknowledge the support of Grant-Aid from Japanese Government for the Scientific research Fund B (2), No.12450075.

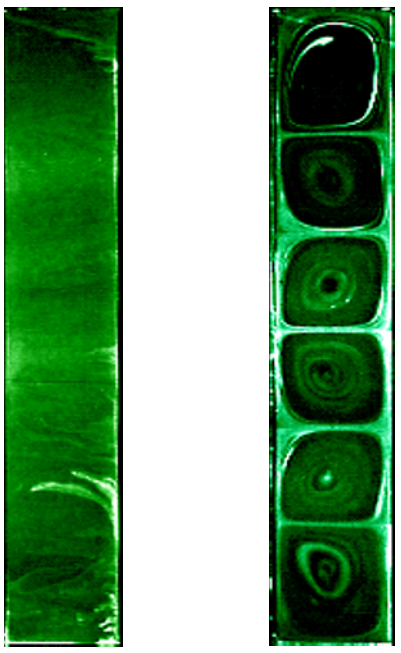

(a) With counter-ion (b) Without counter-ion

Fig. 8. Effect of counter-ion
(*Ta** = 101, *dTa** /*dt* =232 min^{-1}, *T* = 20℃).

References

Arora, K., et al., Surfactant-induced effects on turbulent swirling flows, Rheol. Act, 41(2002), 25-34.
Coles, D., Transition in circular Couette flow, J. Fluid Mech., 21-3(1965), 385-425.
Groisman, A. and Steinberg, V., Couette-Taylor Flow in a Dilute Polymer Solution, Physical Rev. Letters, 77-8 (1996), 1480-1483.
Gupta, V. K., Sureshkumar, R. and B. Khomami, Centrifugal instability of semidilute non-Branian fiber suspensions, Phys. of Fluids, 14-6 (2002), 1958-1969.
Imai, S. and Shikata, T., Viscoelastic Behavior of Surfactant Threadlike Micellar Solutions, Effect of Additives 3, J. Colloid Interface Sci., 244 (2001), 399-404.
Larson, R. G., et al., A purely elastic instability in Taylor-Couette flow, J. Fluid Mech., 218 (1990), 573-600.
Lee, S H.-K., et al., Effect of polymer additives on Görtler vortices in Taylor-Couette flow, J. Fluid Mech., 282 (1995), 115-129.
Ohlendolf, D., et al., Surfactant systems for drag reduction physico-chemical properties and rheological behavior, Rheol. Acta., 25 (1997), 468-486.
Sadanandan, B. and Sureshkumar, Viscoelastic effects on the stability of wall-bounded shear flows, Phys. of Fluids, 14-1 (2002), 41-48.
Snyder, H. A., Wave-number selection at finite amplitude in rotating Couette flow, J. Fluid Mech., 35-2 (1969), 273-298.
Sureshkumar, R., et al., Non-axisymmetric subcritical bifurcations in viscoelastic Taylor-Couette flow, Proc. Roy. Soc. London. A 447 (1994), 135-153.
Taylor, G. I., Stability of a viscous liquid contained between two rotating cylinders, Phil. Trans. Roy. Soc. Lond. A223 (1923), 289-343.
Wei, T., et al., Görtler vortex formation at the inner cylinder in Taylor-Couette flow, J. Fluid Mech., 245 (1992), 47-68.
Zakin, J. L. and Chang, J. L., Polyoxyethylene Alcohol Non-Ionic Surfactants as Drag Reducing Additives, Proc. of Inter. Conf. on Drag Reduction (Cambridge), BHRA. (1974-9), D1-1~D1-14.

Author Profile

Keizo Watanabe: M. Sc. (Eng) in Mechanical Engineering in 1951 from Tokyo Metropolitan University. He also received his Ph.D. in Mechanical Engineering in 1977 from Tokyo Metropolitan University. He worked in Department of Applied Chemical Engineering, University of Toronto as a visiting scholar in 1994. He works in Thermal and Fluid Engineering Division, Tokyo Metropolitan University as a professor since 1989. His research interests are Non Newtonian Fluid Flow, Liquid-Solid Multiphase Flow and Drag Reduction.

Tukasa Takayama: M. Sc.(Eng) in Mechanical Engineering in 2002 from Tokyo Metropolitan University. He works in Research and Development Center of Toshiba Carrier Corporation. He works as a researcher and engineer in next generation technology of air conditioner.

Satoshi Ogata: M. Sc. (Eng) in Mechanical Engineering in 1997 from Tokyo Metropolitan University. He also received his Ph.D. in Mechanical Engineering in 1999 from Tokyo Metropolitan University. He works in Thermal and Fluid Engineering Division, Tokyo Metropolitan University as a research associate since 1999. His research interests are Fluid Rheology, Boundary Layer Flow and Drag reduction.